Water SA 48(3) 304–316 / Jul 2022
https://doi.org/10.17159/wsa/2022.v48.i3.3959

Research paper

Removal of Pb^{2+} ions from synthetic wastewater using functionalized multi-walled carbon nanotubes decorated with green synthesized iron oxide–gold nanocomposite

Balamlile Z Zondo[1], Olawumi O Sadare[1], Geoffrey S Simate[2] and Kapil Moothi[1]

[1]Department of Chemical Engineering, Faculty of Engineering and the Built Environment, Doornfontein Campus, University of Johannesburg, PO Box 17011, Johannesburg 2028, South Africa
[2]School of Chemical and Metallurgical Engineering, Faculty of Engineering and the Built Environment, University of the Witwatersrand, Johannesburg, Private Bag 3, Wits 2050, South Africa

Purification of wastewater before it is discharged into the aquatic environment is important in order to prevent pollution of clean water. This study investigated the applicability of functionalized multi-walled carbon nanotubes (MWCNTs) decorated with gold-iron oxide nanoparticles for the adsorptive removal of Pb^{2+} from synthetic wastewater. CNTs were commercially obtained and functionalized with a mixture of H_2SO_4/HNO_3 acids. The CNTs were coated with gold-iron oxide nanoparticles, to enhance the adsorption of heavy metals. The gold-iron oxide nanoparticles were synthesized by reacting green tea leaf extract with iron chloride ($FeCl_2$) and gold (III) chloride ($HAuCl_4$) precursors. The composite was cross-linked using N, N-dimethylformadide (DMF). The adsorbents were characterized using scanning electron microscopy (SEM) and transmission electron microscopy (TEM) to assess their surface morphology, Fourier transform infrared (FTIR) spectroscopy to identify the functional groups present, X-ray diffraction (XRD) to ascertain the crystallographic structure of the green adsorbent and Raman spectroscopy to determine the sample purity. SEM results showed highly agglomerated and polydispersed nanoparticles, owing to the presence of phytochemicals in the tea extract and magnetic interaction between the individual particles indicating the successful synthesis of Au/Fe_3O_4 adsorbent. Furthermore, an increase in the amount of Pb^{2+} removed per unit mass (q_e) of adsorbent from 1.233 to 7.266 mg·g^{-1} at 298 K was observed. A high sorption capacity was noticed for MWCNT-Au/Fe_3O_4 as compared to the MWCNT-COOH. The Pb^{2+} removal percentage increased from 50% to 78% with an increase in MWCNT-Au/Fe_3O_4 dosage from 0.02 g to 0.1 g. Adsorption isotherm data fitted well to the Freundlich and Langmuir isotherm models for MWCNT-COOH and MWCNT-Au/Fe_3O_4 adsorbents and the rate of Pb(II) adsorption by MWCNT-Au/Fe_3O_4 encountered an increase with increasing solution temperature and followed the pseudo-second-order model. The synthesized MWCNT-Au/Fe_3O_4 has good potential in removing heavy metals from wastewater.

CORRESPONDENCE
Kapil Moothi

EMAIL
kmoothi@uj.ac.za

DATES
Received: 25 October 2021
Accepted: 28 June 2022

KEYWORDS
MWCNT-Au/Fe_3O_4 nanocomposite
wastewater treatment
heavy metals
lead ions

INTRODUCTION

Water pollution by heavy metals has been a great concern for the environment. The term 'heavy metal' refers to metallic elements with high densities, which are highly toxic even at low concentrations (Tchounwou et al., 2012). These include toxic metals such as lead (Pb), copper (Cu), chromium (Cr), mercury (Hg), zinc (Zn), nickel (Ni), cadmium (Cd), and arsenic (As). Heavy metal ions at high concentrations are very harmful and toxic to humans and aquatic life, because they do not degrade into harmless end-products such as organic pollutants (Akpor and Muchie, 2010). Lead, in particular, is one of the most toxic metals found in the release of industrial effluent arising from battery manufacturing, paints, ceramics, glassware, petroleum, rubber and printing press industries (Burakov et al., 2018). The removal of these toxic materials from wastewater is necessary for health and environmental protection. Lead exposure can cause a variety of health problems, such as failure of kidneys, blood disorders, and loss of appetite and reduced fertility in both men and women (Yarkandi, 2014). According to the United States Environmental Protection Agency (USEPA), the maximum recommended level of lead in drinking water is 0.015 mg·L^{-1} (Sharma and Bhattacharya, 2017).

Therefore, it is necessary to develop a simple, effective and efficient technique for the removal of toxic heavy metals present in drinking water. In recent years, a number of conventional methods such as electrochemical treatment (Liu et al., 2013), chemical precipitation (Pahl, 2020), reverse osmosis (Thaci and Gashi, 2019), ion exchange (Zewail and Yousef, 2015), membrane filtration (Alkhudhiri et al., 2020) and adsorption (Alguacil et al., 2018) have been employed for the removal of lead ions from wastewater (Arbabi et al., 2015). However, limitations such as operational costs, low adsorption capacities, and generation of a large volume of rejected residuals, hinder their application (Barakat, 2011; Kanamarlapudi et al., 2018). Among these, adsorption associated with the green synthesis of nanomaterials is considered to have good potential in removing toxic pollutants due to its high removal efficiency, cost-effectiveness, and simplicity in operation; most importantly these offer the possibility of adsorbent regeneration for reuse (Bao et al., 2013). The green synthesized adsorbents are said to be eco-friendly materials and consume less energy during manufacturing (Kharissova et al., 2013).

In recent studies, lead (II) ions have been successfully removed from wastewater via adsorption using green synthesized nanoparticles (Azizi et al., 2017; 18; Mahmoud et al., 2021). Several low-cost natural adsorbents have been reported for lead (II) ion removal – these include: rusk husk (Kulkami, 2016),

palm oil fibre (Nwabanne and Igbokwe, 2012), velvet tamarind (*Dialium indum*) shells (Akoji, 2019), egg shells (Arunlertaree et al., 2007), date trees (Boudrahem et al., 2011), elemi seed, mucuna shell and oyster shell (Okolo et al., 2020). Nanocomposites (Tao et al., 2020), polymers (Mahmud et al., 2014), activated carbon (Alguacil et al., 2018; Zafarzadeh et al., 2018), zeolite (Pandey et al., 2015; Dawagreh et al., 2017; Elboughdiri, 2020), silica gel (Li et al., 2019) and other materials such as carbon nanotubes (CNTs) have all been studied as possible adsorbents for the removal of contaminants from wastewater (Ouni et al., 2019). However, CNTs are considered as the preferred adsorbents in many applications such as inorganic and/or organic pollutants removal, because they possess high surface area and porosity and can be easily modified to possess expected functional groups.

Researchers' attention has been drawn toward utilizing CNTs decorated with nanomaterials as they show superior properties and potential for increasing the adsorption of heavy metals compared to traditional adsorbents (Abhari et al., 2020). However, the application of CNTs in aqueous solution is hindered by their poor dispersion due to the hydrophobicity of their graphitic surface, which can cause loose bundles that reduce the effective surface area (Vukovic et al., 2011). Other drawbacks of using CNTs include low removal efficiency and limited selectivity. In addition, the sorption capacities for heavy metal ions of raw CNTs are very low and require surface modification (Ray and Shipley, 2015). It is therefore essential to address these drawbacks and enhance CNT performance, by functionalizing them using chemical treatment methods and coating with metal/metal oxide for the purpose of improving the adsorption capacity, due to changes to the surface morphology and modification of the surface functional groups (Han et al., 2006). To address this identified research gap, Au/Fe_3O_4 nanoparticles were synthesized using green tea extracts and then incorporated into functionalized multi-walled carbon nanotubes (MWCNT-COOH) for the first time, in order to increase the hydrophilicity, improve dispersability, magnetic properties and the surface area.

Nanomaterials have gained a lot of attention, especially in environmental applications, due to their unique properties, such as nanoscale (1–100 nm) size and high surface area (Sarma et al., 2019). Titanium nanoparticles are well known for their ability to degrade organic pollutants (Menesi et al., 2008). Studies conducted by Nosaka et al. (2005) and Orlov et al. (2007) showed that titanium nanoparticles act as a reaction catalyst for pollutants in water in the presence of UV light. Gold metal (Au) has potential in dealing with water pollution problems such as heavy metals, detergents and fertilizers. In water treatment applications, gold nanoparticles (Au-NPs) are well known for contaminant detection and removal due to their unique properties, such as high surface area per volume, ease of surface modification and high stability (Qian et al., 2013). In addition, they are easy to synthesize and have a strong surface plasmon resonance (SPR). Au-NPs have emerged as promising nanoparticles for detecting the concentration of certain toxic heavy metal ions in water. The advantages of stability and compatibility with aqueous mediums has made them preferred candidates in sensing and detection of water contaminants (Priyadarshini and Pradhan, 2017). Bindhu and Umadevi (2014) synthesized Au-NPs using *Hibiscus cannabinus* leaves with no additional chemical agents and used it to detect Fe^{3+} in water. In recent years, gold nanoparticles have received much interest in the removal of water pollutants. The high specific area of Au-NPs gives high adsorption capacity as compared to other conventional adsorbents (Nitti, 2014).

In this study, Au-NPs were synthesized using green tea extract, which contains a high amount of polyphenols. The -OH group is responsible for the reduction of $[AuCl_4^-]$ while the -COO- group is responsible for stabilization of the Au-NPs formed. Iron oxide–based materials have received great recognition for heavy metal removal from wastewater in recent years. Iron oxides exist in various forms in nature, as magnetite (Fe_3O_4), hematite (α-Fe_2O_3), and maghemite (γ- Fe_2O_3) (Islam et al., 2012). Magnetite is an attractive adsorbent for the removal of heavy metals due to its large surface area, reusability, super-magnetic properties, low cost, and ease of synthesis. However, iron oxides are unstable due to their ability to undergo oxidation easily. To overcome this issue, a combination with a noble metal such as gold (Au) or silver (Ag) has been reported (Fodjo et al., 2017). In addition to gold and iron oxide–based nanoparticles, silver nanoparticles are of great interest due to their antibacterial activity, rather than their use in heavy metal removal.

Based on this background, this study focused on the applicability of CNTs decorated with Au/Fe_3O_4 nanocomposites synthesized via the green route as adsorbents for removal of Pb (II). This was achieved by anchoring functional groups onto the sides/walls of CNTs to increase the activity of tubes towards the removal of heavy metal ions from aqueous solutions (Soni et al., 2020). In addition, kinetics studies were carried out to better understand the adsorption mechanisms and the interaction between adsorbents and adsorbates.

MATERIALS AND METHODS

All chemicals used were of analytical or reagent grade and were used as obtained from the suppliers. The green tea leaves were purchased from a tea merchant in Johannesburg, South Africa. Raw multi-walled carbon nanotubes (MWCNTs) >95% purity, with an outer diameter (OD) ranging from 10–20 nm and 30 nm in length, and gold (III) chloride 99.995% were purchased from Sigma Aldrich Pty (Ltd), Johannesburg, South Africa. Nitric acid (HNO_3) 65% purity, sulphuric acid (H_2SO_4) 98% purity, dimethyl formamide (DMF), sodium hydroxide (NaOH), lead nitrate $Pb(NO_3)_2$, and MWCNTs >95% were all purchased from Associated Chemical Enterprise (ACE), Johannesburg, South Africa. Potassium bromide extra pure, 99.5%, and iron (II) chloride ($FeCl_2$) were purchased from Protea Laboratory Solutions (Pty) Ltd.

Preparation of green tea leaf extract

About 5 g of green tea leaves were added to a flask containing 150 mL of distilled water. The solution was heated at 80°C in a hot water bath for 1 h to brew the tea in order to get the tea extract. The filtrate was obtained by filtering using 0.45 µm filter paper and kept on a rotary shaker for 60 min to allow for cooling and further use in nanoparticle synthesis. The pH of the tea extract was determined at almost neutral ~6.5. The prepared tea extract serves as a reducing agent in the synthesis of nanoparticles (Fayemiwo et al., 2018).

Synthesis of Au-coated iron oxide nanoparticles

A 0.01 M stock solution was prepared by mixing 0.0162 g of $FeCl_2$ in 10 mL of distilled water. The stock solution was diluted to 0.001 M strength for the synthesis of iron oxide nanoparticles in 10 mL solution. The amount of 1 mL of the stock solution was added to 7.5 mL of water and stirred for 5 min, after which 1.5 mL of tea extract was added (0.15% (w/v) strength of tea). Additionally, the colour of the solution changed from yellow to a dark green-black colour, immediately confirming the synthesis of iron oxide nanoparticles at ambient temperature. Thereafter, about 10 mL of 0.01 M $HAuCl_4$ was added to the solution with the tea, so that it would be reduced and coated on the iron oxide nanoparticles. The synthesized nanoparticles were centrifuged and washed with distilled water and ethanol to remove excess precursors or

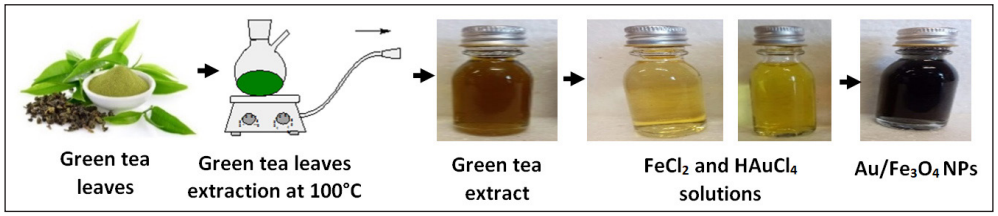

Figure 1. Synthesis of Au and Fe_3O_4 nanoparticles

polyphenols present. A black substance was obtained at the end of the synthesis, and dried in an oven for 60 min to reduce its moisture content. The samples were then kept in a closed glass container for SEM characterization. Figure 1 summarizes the synthesis process of Au/Fe_3O_4 nanoparticles.

Functionalization of MWCNTs to prepare MWCNT-COOH

CNTs contain a high level of impurities, such as carbon or residual metal nanoparticles found from the catalyst used in the synthesis process. The purification of CNTs is achieved by washing them with a nitric acid solution to open their closed ends, which makes them unreactive. CNTs were functionalized using acid oxidation treatments to introduce oxygen-containing functional groups (hydrophilic groups of carboxylic acid) to their walls and to enhance their solubility, reactivity and dispersion of CNTs in aqueous solution. These functional groups act as an anchor site for metal ions on CNTs. Raw CNTs are hydrophobic and after functionalization are said to be hydrophilic (Fig. 2). The oxidation of MWCNTs was carried out as reported by Haider et al. (2015). Raw-CNTs (0.1 g) were dispersed in a round-bottomed flask containing a mixture of concentrated sulfuric acid 95% (H_2SO_4) and nitric acid (65% HNO_3) at 3:1 under ultra-sonication technique for 3 h to remove residual metal impurities from the tubes and produce oxidized CNTs (CNT-COOH). The resulting solution was filtered, and the solid was washed continuously with deionized water until neutral pH was obtained. The sample was dried at 70°C for 24 h. Figure 2 shows the samples of as-received and functionalized CNTs in water.

Preparation of MWCNT-Au/Fe_3O_4 nanocomposite

About 0.1 g CNTs were mixed with 10 mL N, N-dimethylformadide (DMF) with constant stirring. About 0.3 g of Au-Fe_3O_4 nanoparticles were added to MWCNT solution. Then, a composite was ultra-sonicated for 1 h to allow the mixture to dissolve, which subsequently resulted in Au/Fe_3O_4 nanoparticles being well coated on the surface of the oxidized CNTs. About 3 mL of the putty form of the CNT-Au/Fe_3O_4 nanocomposite was dried at 25°C overnight for the solvent to evaporate. The synthesized CNT-Au/Fe_3O_4 nanocomposite adsorbent was characterized and kept for use in the treatment of Pb-containing wastewater.

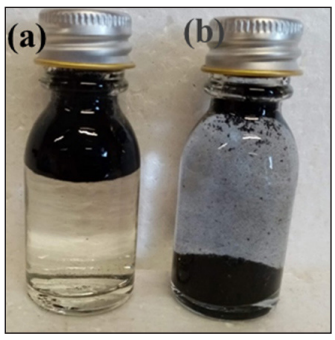

Figure 2. (a) Raw-MWCNTs and (b) MWCNT-COOH

Characterization techniques

The morphology (shapes and sizes) of a synthesized nanocomposite was investigated using TEM JEM-2100 JEOL operated at 200 kV and the elemental composition was obtained using the Oxford INCA EDS detector system coupled with TEM. Samples were prepared by diluting a few milligrams of a sample with ethanol, dropped on a carbon-coated copper grid and allowed to dry at room temperature. Scanning electron microscopy (SEM) analysis was carried out using SEM JOEL JSM-5600. The samples were coated with carbon in order to avoid charging and to attain better images. X-ray diffraction (XRD) analysis was performed on pulverized samples using a Bruker XRD machine carried out in the two theta (2θ) on a D8 diffractometer. The functional groups on the surface of the nanocomposite were detected using a Perkin-Elmer Spectrum: Model 1000 series Fourier transform infrared spectrometer (FTIR). A small amount of powder sample, just enough to cover the tip of a spatula, was mixed with KBr powder. Then, the mixture was ground for 5 min in a mortar to fine powder. The specimen was then put into the sample holder for analysis. Spectra were collected over the range of 400–4 000 cm^{-1}. The information on the structure, purity and crystallinity of the adsorbent was obtained using a Jobin-Yvon T64000 Raman Spectrometer. The intensity measurement of scattered light as a function of its frequency produces a Raman spectrum and the purity, crystallinity arrangement of CNTs were evaluated based on the ratio of the intensity of the disorder/defect (I_D) and graphitic (I_G) bands. The textural properties of the adsorbents (surface area, pore volume and pore size) were obtained using Brunauer-Emmet and Teller (BET) through gas adsorption. Nitrogen gas at 77 K was used to obtain the adsorption data.

Preparation of synthetic water and the removal of Pb (II) ions using MWCNT-Au/Fe_3O_4 nanocomposite

The adsorption of Pb^{2+} on MWCNT-Au/Fe_3O_4 was investigated by using batch adsorption experiments. Synthetic water was prepared using Pb $(NO_3)_2$. About 1.615 g of 99% Pb $(NO_3)_2$ was dissolved in distilled water in a 1 L beaker to obtain 1 000 ppm ($mg{\cdot}L^{-1}$) of lead stock solution. Batch adsorption studies were performed by mixing 0.5 g of composite with 50 mL solutions containing different lead ion concentrations (2, 4, 6, 8 and 10 $mg{\cdot}L^{-1}$) in a 100 mL volumetric flask/beaker and the pH value was adjusted using 0.5 M H_2SO_4 or 0.5 M NaOH. The samples were filtered with 0.45 µm Whatman filter paper. Final concentrations of the samples were detected using a Thermo Fisher ICE 3300 Flame Atomic Adsorption Spectrometer (FAAS) (Hassan and Mahdi, 2016).

The amount of metal ion adsorbed on the composite, q_e ($mg{\cdot}g^{-1}$) was determined using Eq. 1:

$$q_e = \frac{(C_o - C_t) \times V}{m} \quad (1)$$

where C_0 ($mg{\cdot}L^{-1}$) and C_t ($mg{\cdot}L^{-1}$) are the initial and final concentrations of pollutant (lead ions) after a certain period of time, respectively, q_e ($mg{\cdot}g^{-1}$) is the amount of pollutant adsorbed, m (g) is the mass of the CNT/Au/Fe_3O_4 composite and V (L) is the volume of the liquid phase.

The percentage removal of lead ions from the solution is calculated using Eq. 2:

$$\%\text{Removal} = \frac{(C_o - C_t)}{C_o} \times 100 \rightarrow R(\%) = \left(1 - \frac{C_t}{C_o}\right) \times 100 \qquad (2)$$

where C_0 and C_t will be the initial and final concentrations of pollutant(s) in the solution, respectively.

Finally, the adsorption isotherms were compared with Langmuir and Freundlich isotherms. The adsorption kinetics were modelled using pseudo-first-order and pseudo-second-order equations. Table 1 provides detailed information on the conditions of the experiment in terms of pH, contact time, adsorbed dosage, and temperature for Pb (II) ion adsorption.

RESULTS AND DISCUSSION

Physicochemical characterization of Au/Fe_3O_4 nanoparticles and MWCNT-Au/Fe_3O_4 nanocomposite adsorbent

Characterization of the Au/Fe_3O_4 nanoparticles using SEM

The surface morphology of Au/Fe_3O_4 nanocomposite was assessed using SEM, as depicted in Fig. 3. The synthesized nanoparticles are highly agglomerated and polydispersed in the aqueous medium due to the phytochemicals present in the extract. The observed morphology of the Au/Fe_3O_4 magnetic nanocomposite was comparable to that previously reported by Ruíz-Baltazar (2021).

Morphology of functionalized CNTs and synthesized nanocomposite adsorbent

Energy dispersive X-ray (EDX) was used to analyse the chemical composition of the synthesized nanoparticles. The EDX spectrum (Fig. 4) presents all the elements found in the MWCNT-Au/Fe_3O_4 and their corresponding atomic weight percentages (C: 62.3%; Fe: 23.6%; O: 8.0%; Au: 4.3% and Cu: 1.8%). The presence of carbon in the EDS analysis is in line with the findings of Fameyiwo et al. (2018), for compounds identified on the GC-MS spectrum of green tea extract, which is rich in carbon and oxygen. The carbon peak could have been obtained from the carbon tape used in mounting the samples.

Table 1. Experimental conditions for adsorptive removal of Pb^{2+}

No.	Parameters	Variations
1	Pb^{2+} stock solution ($mg{\cdot}L^{-1}$)	2–10
2	Adsorbent dosage (g)	0.02–0.12
3	pH values	1–10
4	Contact time (min)	10–240
5	Agitation speed ($r{\cdot}min^{-1}$)	160
6	Volume (mL)	50

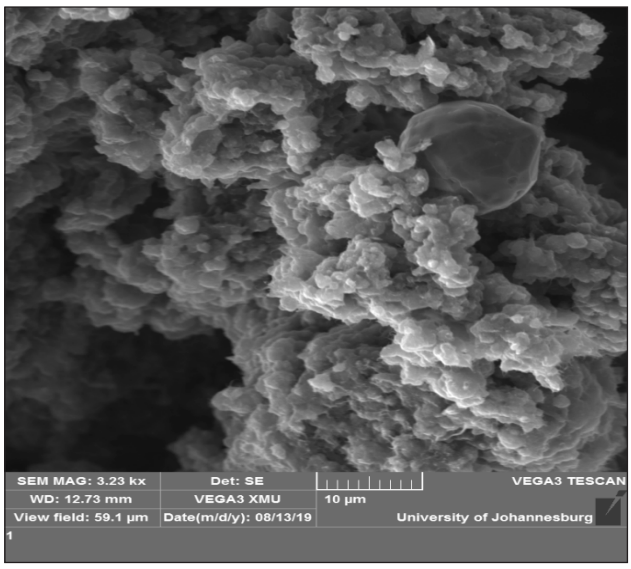

Figure 3. SEM image of Au/Fe_3O_4 (10 µm magnification)

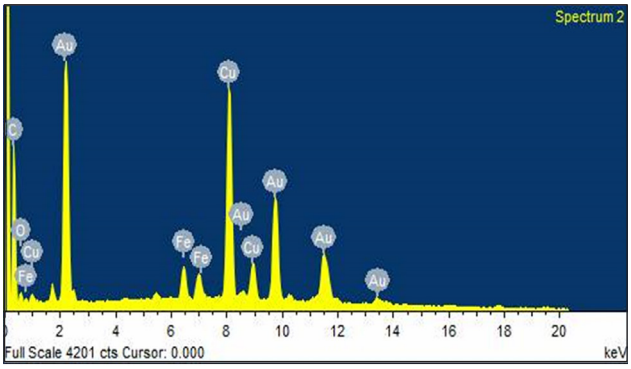

Figure 4. EDS spectrum and elemental composition of MWCNT-Au/Fe_3O_4

To assess the morphology and internal structure of the adsorbents, TEM characterization was performed. Figures 5a and 5b show the TEM images of raw-MWCNT and F-MWCNT (MWCNT-COOH), respectively. Figures 5c and 5d depict the synthesized Au/Fe_3O_4-MWCNT nanocomposite at different magnifications. F-MWCNT appear more spaced and less packed compared to raw-MWCNT. This could be as a result of functionalization. In addition, impurities were observed on the surface of the as-received MWCNTs (see Fig. 5a, with broken red circle). However, Fig. 5b showed a neater TEM image of the CNTs after functionalization. This is an indication that functionalization of MWCNTs removes impurities such as carbon residues. In Figs 5c and 5d, the uniform pattern of Au/Fe_3O_4 nanoparticles can be observed, as well as their attachment on the walls of the CNTs. It can be seen that the distribution of Fe_3O_4/Au on the surface of F-MWCNT is uniform and the surface of F-MWCNT became courser after loading with nanoparticles. Aslam et al. (2021) obtained similar images of raw and functionalized CNTs.

Surface functionalities of f-MCNTs and nanocomposites adsorbent

Figure 6 depicts the surface chemical functionalities of the f-MCNTs and the MWCNT-Au/Fe_3O_4 nanocomposite adsorbent. The peaks ascribed in the range of 1 500–1 717 cm^{-1} correspond to the C=O stretching of COOH, indicating the presence of new groups formed after oxidation. Furthermore, the band in the range of 1 000 – 1 011 cm^{-1} is attributed to the C–O stretching, while the wide band beyond 3 000 cm^{-1} indicates the presence of O–H groups, showing water molecules. The peak observed at around 2 958 cm^{-1} represents C-H stretching. The FTIR spectra of f-MWCNTs have observations similar to those previously reported by Aslam et al. (2021). In the FTIR spectrum of MWCNT-Au/Fe_3O_4, new peaks around 550–1 550 cm^{-1} could be attributed to the stretching vibration of Fe–O and Au–O, which confirms that Au/Fe_3O_4 was loaded onto the surface of MWCNT-COOH. This study confirms the results obtained in previous research (Fayemi et al., 2015; Tehrani et al., 2014).

Purity of f-CNTs and MWCNT-Au/Fe_3O_4 nanocomposites

Figure 7 shows the Raman spectra of the adsorbent samples. Two main peaks in the Raman spectra appeared in the samples at 1 500 and 2 500 cm^{-1}, known as D and G bands, respectively. The D band is related to the disorderly carbon atoms of MWCNTs, corresponding to sp^3 hybridized, and the G band indicates sp^2 hybridized carbon sheets. The area ratio of the D to G bands (I_D/I_G)

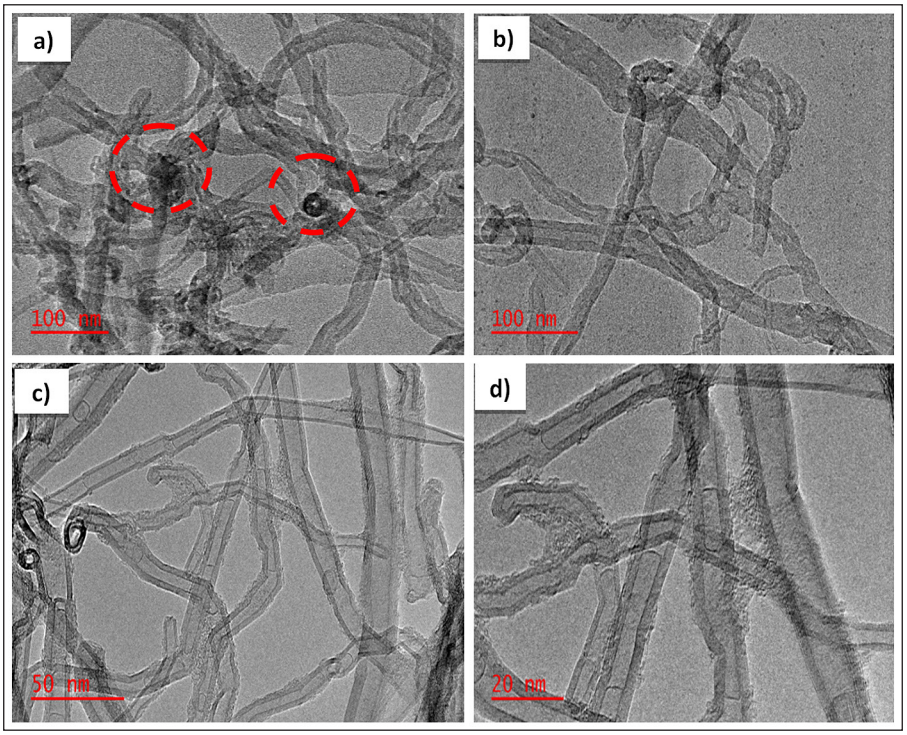

Figure 5. Morphological structure of (a) raw-MWCNT, (b) MWCNT-COOH, (c) and (d) MWCNT-Au/Fe_3O_4

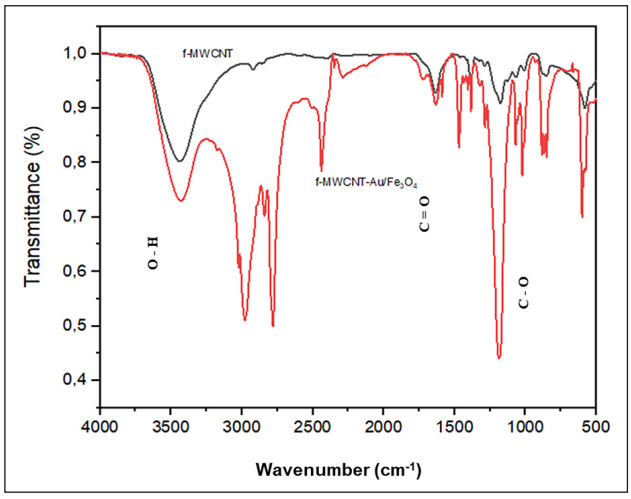

Figure 6. FTIR spectra of f-MWCNT and MWCNT-Au/Fe_3O_4 nanocomposite

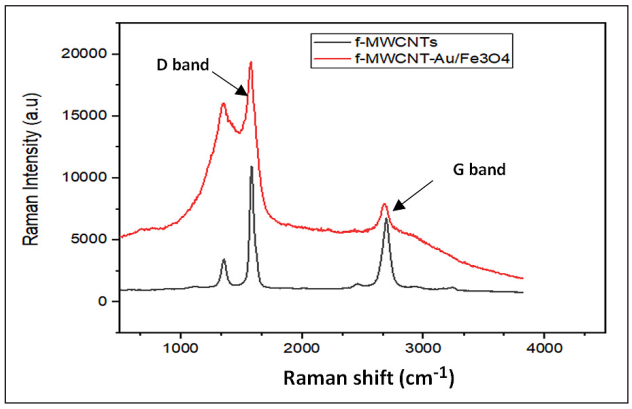

Figure 7. Raman shift of f-MWCNT and fMWCNT-Au/Fe_3O_4

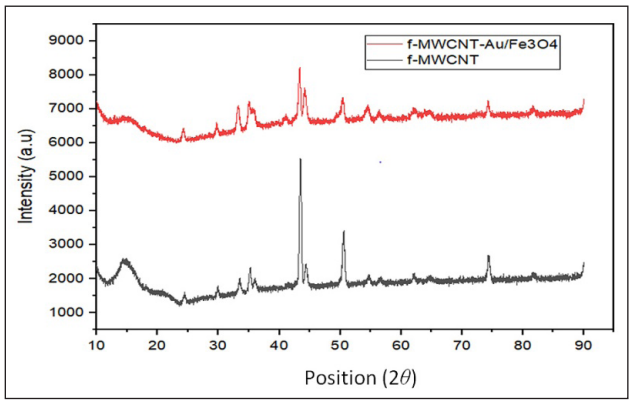

Figure 8. XRD pattern of f- MWCNT and MWCNT-Au/Fe_3O_4 nanocomposite

can be used to assess the amount of defects in nanomaterial structures. Due to the elimination of amorphous carbon during acid treatment, the ratio of f-MWCNTs was 1.6 (I_D/I_G = 1.67), whereas a higher ratio of 2.67 (I_D/I_D = 2.67) was obtained for MWCNTs-Au/Fe_3O_4. This could be an indicator for successful conversion of f-MWCNTs to fMWCNTs-Au/Fe_3O_4 (Dehaghi, 2014).

Crystallinity of f-MCNTs and MWCNT-Fe_3O_4/Au nanocomposites

The crystallinity of the functionalized MWCNT and MWCNT-Au/Fe_3O_4 composites were further evaluated using XRD analysis. Figure 8 shows the XRD pattern of the synthesized samples. The strong diffraction peak of f-MWCNT is observed at $2\theta = 45°$. After the deposition of Fe_3O_4/Au nanoparticles, new diffraction peaks revealed the crystallinity of Fe_3O_4/Au specimens with different diffraction peaks located at $2\theta = 35°$, 46°, 50°, 55° and 75°, although there was a slight difference in diffraction peaks formed between the two samples, which was caused by the method (green method) used in depositing the nanoparticles. The XRD results obtained still confirmed that the Fe_3O_4/Au nanoparticles were successfully coated on the walls of f-MWCNT.

Textural properties of raw-MWCNT, MWCNT-COOH and MWCNT-Au/Fe_3O_4

The textural properties of the adsorbents (surface area, pore volume and pore size) obtained from BET analysis are presented in Table 2. An increase in surface area and pore volume of MWCNT-Au/Fe_3O_4 was noted due to increasing functionalization of MWCNT-COOH. The results shown in Table 2 confirm that surface area and pore volume of nanomaterials can be increased based on the extent of functionalization of MWCNT-COOH and MWCNT-Au/Fe_3O_4, which possesses a large surface area and increased pore volume. As such, it is capable of enabling faster and better sorption ability of the adsorbents for the removal of Pb^{2+} from aqueous solutions. Even though a slight increase in pore volume and pore size was obtained, the composite could possess the capability of absorbing contaminants in water. Similarly to the results obtained in this study, Rodriguez et al. (2020) showed an increase in BET surface area from 157.34 to 179.53 $m^2 \cdot g^{-1}$ with MWCNTs treated with HNO_3. The increase in surface area suggests that acid-functionalized MWCNTs have better potential as an adsorbent compared to raw MWCNTs (Rodriguez et al., 2020).

Zeta-potential measurements

Raw carbon nanotubes are well known to have an isoelectric point in the pH range of 5–8 and the isoelectric points of the purified carbon nanotubes (MWCN-COOH) shift to the lowest pH values because of the presence of the acidic groups (Swarek et al., 2016). Lu and Chiu (2008) reported that the increase in pH of the solution is caused by the charge on the surface of MWCNTs, which is due to the deposition of hydroxide ions on the MWCNT surface. The surface chemistry of MWCNT-Au/Fe_3O_4 nanocomposite was studied using the Malvern zetasizer (Fig. 9). The point of zero charge (pH_{pzc}) was used to investigate whether the surface of the nanocomposite had polar functional groups attached. Appel et al. (2003) proposed a number of methods for determining pH_{pzc} in materials, such as non-specific ion adsorption, potentiometric titration, and methods that are based on the mobility of charged particles. However, most of the research on nanocomposite materials has focused on the use of the solid addition method due to its simplicity. The zeta-potential was measured at pH 2, 4, 6, 8 and 10. The oxidized MWCNTs and MWCNT-Au/Fe_3O_4 exhibit a negative charge in this pH range and therefore the zeta potential values increase with increase in pH due to the breaking down of ions that convey the negative charge to the carbon nanotube surface.

Batch adsorption experiments

Batch adsorption experiments were carried out to examine the effectiveness and efficiency of MWCNT-COOH and MWCNT-Au/Fe_3O_4 for the removal of Pb^{2+} from water. The role of various parameters that influence adsorption, such as pH, contact time, adsorbent dose, temperature, and initial adsorbate concentration, were investigated to determine the most suitable conditions for Pb^{2+} removal. The data obtained were modelled with various kinetic and isotherm models in order to find the one that best describes the adsorption process.

Effect of pH

The influence of pH on Pb^{2+} adsorption was investigated using MWCNT-COOH and MWCNT-Au/Fe_3O_4 over a pH range of 1–10. Figure 10 shows the influence of pH on the adsorption of Pb^{2+}. High removal efficiencies were observed as the pH solution increased, but a sharper increase was observed for MWCNT-Au/Fe_3O_4 because of the chemical interaction between the metal ions and functional groups found on the surface, which are carboxyl (–COOH), hydroxyl (–OH) and carbonyl (–C=O). This attachment of the functional groups and Au/Fe_3O_4 nanoparticles improved the adsorption capacity of Pb^{2+} in solution. Moreover, as the pH increases (in basic conditions), the charge of the MWCNT surface becomes more negative, causing electrostatic interactions between cationic metal ions and negatively charged surfaces of both adsorbents, and resulting in higher Pb^{2+} adsorption. Hamza et al. (2013) and Elham et al. (2010) reported a similar observation for Pb^{2+} adsorption. The adsorption capacity of Pb^{2+} increased even at higher pH values, up to pH 10. Therefore, pH 7 was selected as the optimum value where maximum adsorption capacity of MWCNT-Au/Fe_3O_4 nanocomposite was achieved while avoiding the chance of precipitation (Hayati et al., 2016).

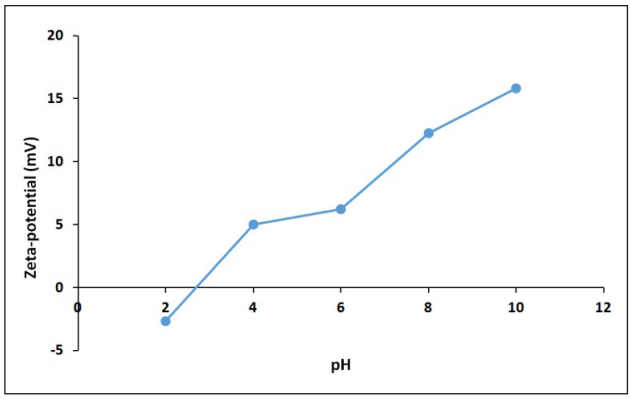

Figure 9. Zeta-potential plot showing the point of zero charges of MWCNT-Au/Fe_3O_4 nanocomposite at various pH values

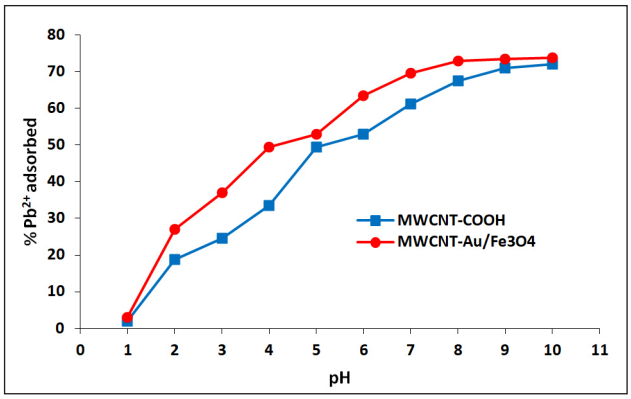

Figure 10. Effect of pH on the adsorption of Pb^{2+} using MWCNT-COOH and MWCNT-Au/Fe_3O_4. Experimental conditions: 1 000 $mg \cdot L^{-1}$ Pb^{2+} concentration, 60 min equilibrium time, 0.1 g adsorbent dose, agitation speed of 160 $r \cdot min^{-1}$, temperature of 298 K

Table 2. The textural properties of raw-MWCNT, MWCNT-COOH and MWCNT-Au/Fe_3O_4 from BET analysis

Adsorbent	Single point surface area ($m^2 \cdot g^{-1}$)	Pore volume ($cm^3 \cdot g^{-1}$)	Pore size (nm)
Raw-MWCNT	44.996	0.358	0.718
MWCNT-COOH	96.705	0.388	0.716
MWCNT-Au/Fe_3O_4	105.027	0.389	0.748

Effect of contact time

Figure 11 shows the influence of varying the contact time on the adsorption of Pb^{2+} using MWCNT-COOH and MWCNT-Au/Fe_3O_4 nanocomposite adsorbents, over a period of 10–240 min. The experimental runs showed that adsorption of Pb^{2+} increased with increasing contact time with these adsorbents. Initially, more Pb^{2+} were adsorbed due to the availability of more active sites, but at a later stage the active sites became saturated, causing less or no increase in removal (Sadare and Daramola, 2019; Sadare et al., 2020). Equilibrium was reached at 100 min for both MWCNT-COOH and MWCNT-Au/Fe_3O_4 for the removal of Pb^{2+}. The study revealed that about 57.54% and 59.97% of Pb^{2+} removal was obtained for MWCNT-COOH and MWCNT-Au/Fe_3O_4, respectively. The slight increase in efficiency of the nanocomposite was attributed to the increased surface area obtained after modification, which created more active sites available for metal ion adsorption. Pandhare et al. (2013) obtained similar results due to some unsaturated adsorption sites during the adsorption reaction.

Effect of adsorbent amount

Figure 12 shows the influence of varying adsorbent amounts on Pb^{2+} adsorption using MWCNT-COOH and MWCNT-Au/Fe_3O_4. The adsorbent dosage was varied over a range of 0.01–0.12 g. Percentage removal initially increases sharply with an increase in adsorbent amount. The Pb^{2+} removal percentage increased from 50% to 78% with an increase of MWCNT-Au/Fe_3O_4 dosage from 0.02 to 0.1 g. The increased adsorbent amount provides the increased surface area, which makes more active sites available. Adebowale et al. (2020) obtained similar results with an increase in adsorption of Pb^{2+} ions.

Effect of temperature

The influence of temperature on Pb^{2+} adsorption was investigated using MWCNT-COOH and MWCNT-Au/Fe_3O_4. This was examined over a range of 293–313 K at varying concentrations of 2–10 mg·dm^{-3}. Figures 13a and 13b show that the adsorption capacities of Pb^{2+} on MWCNT-COOH and MWCNT-Au/Fe_3O_4 were observed to increase with increasing temperatures; this was due to increased kinetic energy, mass transfer and metal ion diffusion to the pores of the adsorbent (Gusain et al., 2019). A slight increase in adsorption capacity (q_e) as the adsorbent concentration increases from 2–10 mg·dm^{-3} was observed. At a temperature of 298 K, an increase in the amount of Pb^{2+} removed per unit mass (q_e) of the adsorbent from 1.78–4.61 mg·g^{-1} and 1.23–7.2 mg·g^{-1} was obtained for MWCNT-COOH and MWCNT-Au/Fe_3O_4, respectively. This could be due to an increase in the force that is needed to overcome the friction on the active sites of the MWCNT-Au/Fe_3O_4 at high Pb^{2+} ion concentration (Oyetade et al., 2016).

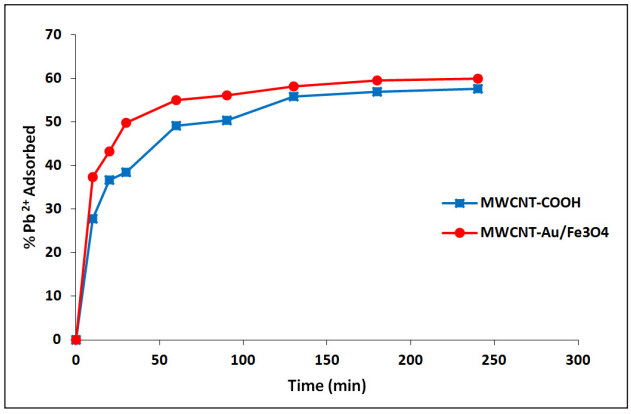

Figure 11. Effect of contact time on the adsorption of Pb^{2+} using raw-MWCNT, MWCNT-COOH, and MWCNT-Au/Fe_3O_4. Experimental conditions: 1 000 mg of·L^{-1} Pb^{2+} concentration, pH 7, 0.1 g adsorbent dose, and agitation speed of 160 r·min^{-1}, temperature of 298 K.

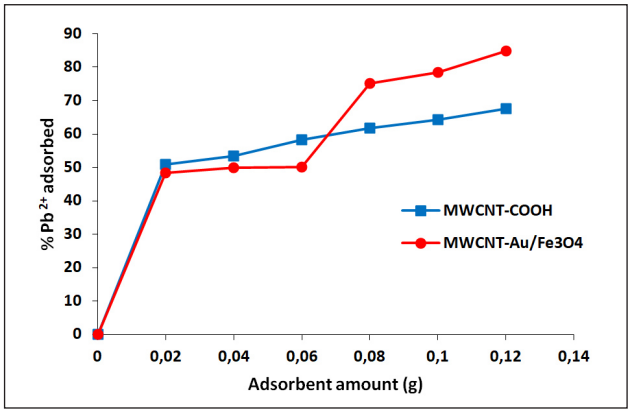

Figure 12. Effect of adsorbent amount on the adsorption of Pb^{2+} using raw-MWCNT, MWCNT-COOH and MWCNT-Au/Fe_3O_4. Experimental conditions: 50 mL of 1 000 mg·L^{-1}, 60 min equilibrium time, agitation speed of 160 r·min^{-1}, temperature of 298 K.

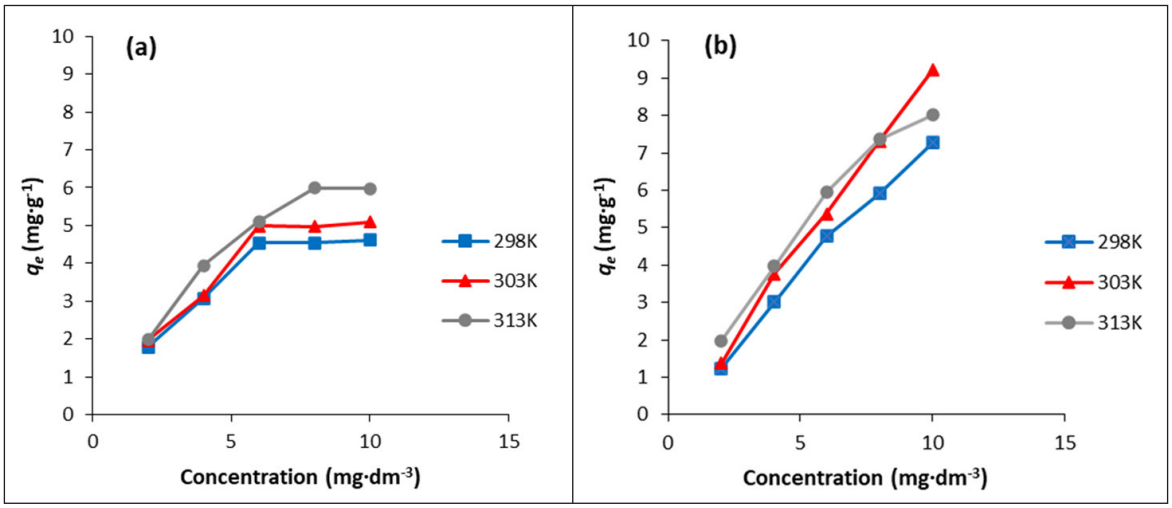

Figure 13. Effect of varying temperature on the adsorption of Pb^{2+}: (a) MWCNT-COOH and (b) MWCNT-Au/Fe_3O_4. Experimental conditions: 60 min equilibrium time, pH 7, agitation speed of 160 r·min^{-1}.

Adsorption kinetics and isotherm studies

Adsorption isotherms

Adsorption isotherms provide information on the amount of adsorbent needed to remove a unit mass of solute per gram of adsorbent, as well as the ability of the adsorbent to remove the pollutant (Sadare and Daramola, 2019). Furthermore, they describe the equilibrium relationship between the adsorbate in the liquid phase and the adsorbate adsorbed on the surface of the adsorbent at constant temperature. In this study, two isotherm models (Langmuir and Freundlich) were applied for the description of the adsorption processes. The Langmuir isotherm is represented in Eq. 3 and Eq. 4:

$$q_e = \frac{q_{\max} \mathrm{K_L} C_e}{1 + \mathrm{K_L} q_{\max}} \tag{3}$$

And linearly:

$$\frac{1}{q_e} = \frac{1}{\mathrm{K_L} q_{\max}} \cdot \frac{1}{C_e} \tag{4}$$

where, q_e is the amount adsorbed per unit mass of adsorbent at equilibrium (mg·g^{-1}), C_e is the equilibrium concentration of adsorbate in solution (mg·dm^{-3}), q_m is the maximum monolayer adsorption capacity (mg·g^{-1}) and $\mathrm{K_L}$ is the Langmuir isotherm constant (dm^3·mg^{-1}).

The characteristics of the Langmuir isotherm may be expressed in terms of the equilibrium parameter R_L, which is known as the separation factor or the equilibrium parameter (Eq. 5).

$$R_L = \frac{1}{1 + K_L C_o} \tag{5}$$

The R_L values indicate that the type of adsorption is either unfavourable ($R_L > 1$), linear ($R_L = 1$), favourable ($0 < R_L < 1$), or irreversible ($R_L = 0$) (Elmi et al., 2017; Sadare and Daramola, 2019).

The Freundlich isotherm describes the equation for non-ideal adsorption that involves heterogeneous adsorption. The Freundlich isotherm is presented in Eq. 6:

$$\log q_e = \log \mathrm{K_F} + \frac{1}{n} \log C_e \tag{6}$$

where $\mathrm{K_F}$ represents the Freundlich isotherm constant (mg·g^{-1}) and n is the adsorption intensity of the relationship between the adsorbate and adsorbent.

Figures 14a and 14b present the Langmuir isotherms MWCNTs-COOH and MWCNT-Au/Fe_3O_4 nanocomposite adsorbents, respectively. Figures 15a and 15b present the Freundlich isotherms for MWCNTs-COOH and MWCNT-Au/Fe_3O_4 nanocomposite adsorbents, respectively. Table 3 presents both Langmuir and Freundlich isotherm parameters. From the values of R^2 obtained in Table 3, it can be concluded that both Langmuir and Freundlich isotherms fitted well for MWCNT-COOH and MWCNT-Au/Fe_3O_4 with a coefficient of determination (R^2) of 0.9944 and 0.9993, respectively. The MWCNT-Fe3O4 was best fitted to a linear regression isotherm. The values of R_L for both

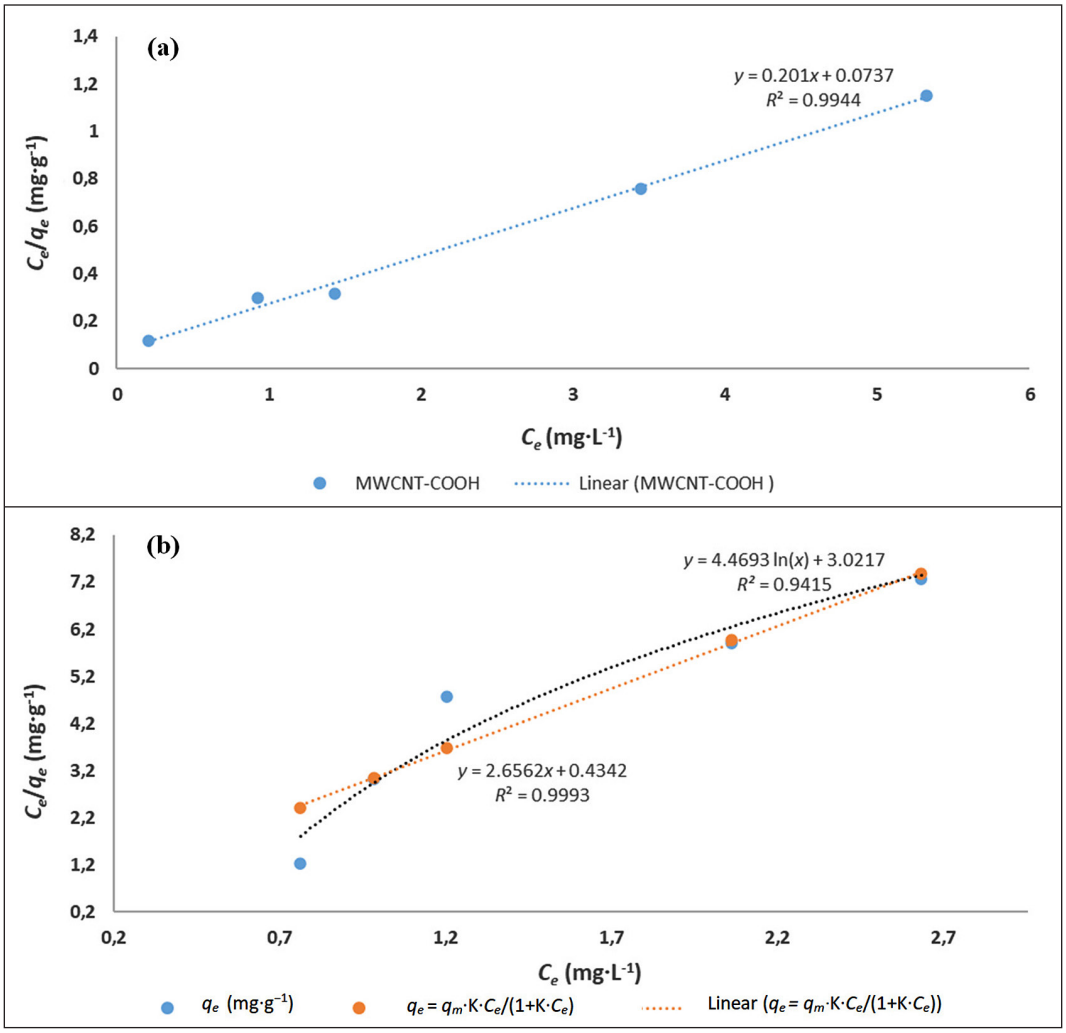

Figure 14. (a) and (b) Plot of Langmuir adsorption linear and non-linear isotherm parameters ($1/C_e$ vs $1/q_e$) for MWCNT-COOH and MWCNT-Fe_3O_4, respectively. Experimental conditions: 0.1 g f-MWCNTs; 60 min reaction time, pH 7 and temperature of 298 K.

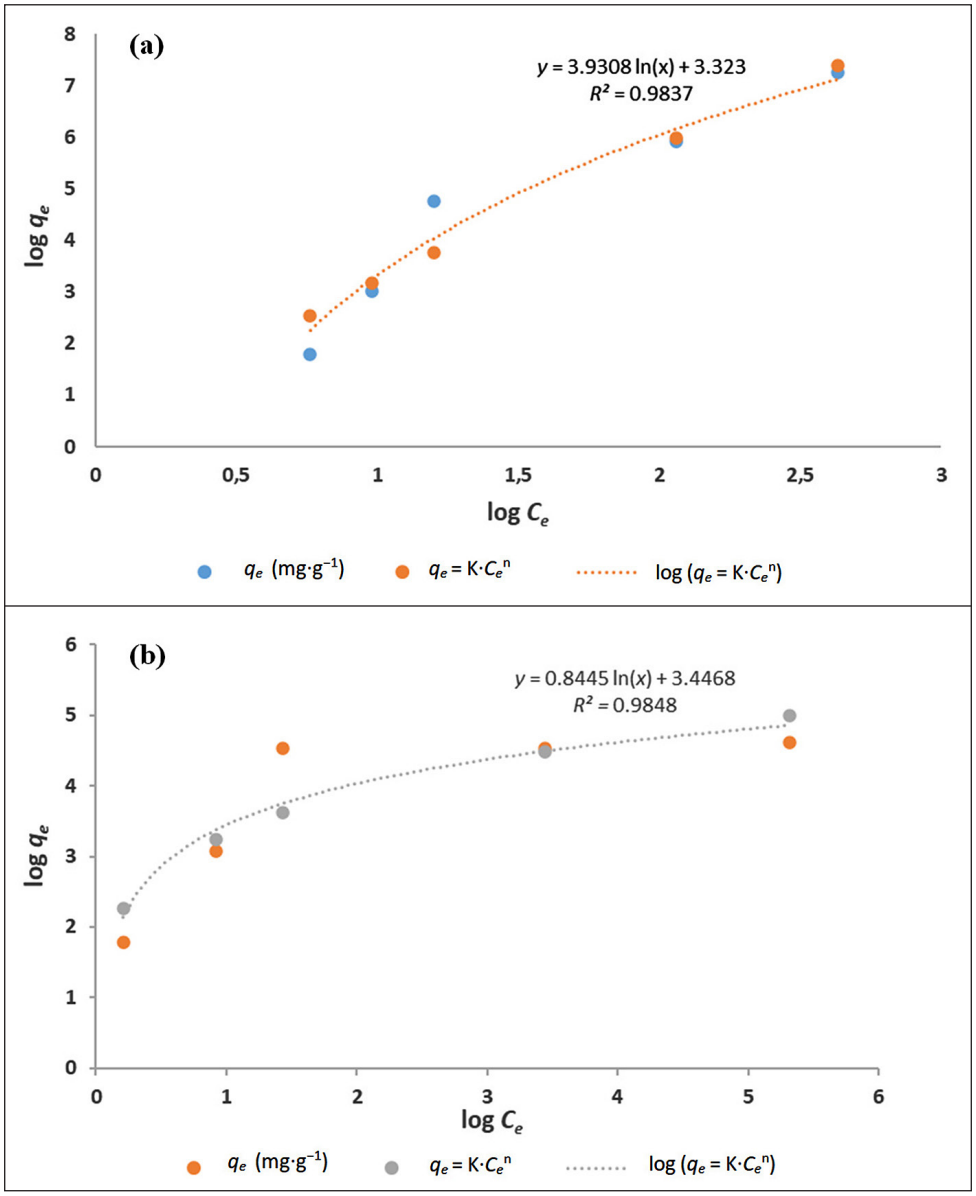

Figure 15. Plot of Freundlich adsorption isotherm parameters (log q_e vs log C_e) for (a) MWCNT-COOH and (b) MWCNT-Au/Fe_3O_4. Experimental conditions: 0.1 g f-MWCNTs; 60 min reaction time, pH 7 and temperature 298 K.

Table 3. Isotherm parameters for the removal of Pb^{2+}

Adsorbent	Isotherms						
	Langmuir				Freundlich		
	q_m (mg·g^{-1})	K_L (L·mg^{-1})	R_L	R^2	K_F	1/n	R^2
MWCNT-COOH	4.9751	0.3667	0.1	0.9944	3.2114	1.1608	0.9837
MWCNT-Au/Fe_3O_4	47.4385	0.0699	0.2	0.9988	3.3119	4.0625	0.948

nanocomposite adsorbents are less than 1, indicating favourable adsorption processes (Elmi et al., 2017; Sadare and Daramola, 2019). The values of q_m and K_L were calculated to be 0.0699 and 47.4385 mg·L^{-1}, respectively.

Adsorption kinetics

Adsorption kinetics were used to examine the nature of the adsorption mechanism involved and also to determine the uptake rate and equilibrium time (Elmi et al., 2017). This knowledge is also useful for the design of future large-scale adsorption facilities. The dynamics of adsorption is investigated by fitting the experimental data obtained to kinetic models. Commonly used kinetic models for solid–liquid adsorption systems are the pseudo-first-order (Eqs 7 and 8) and pseudo-second-order.

The pseudo-first-order:

$$\frac{d_q}{d_t} = k_1(q_e - q_t) \quad (7)$$

$$\ln(q_e - q_t) = \ln q_e - k_1 t \quad (8)$$

where q_t and q_e are the quantities of pollutants adsorbed at any time t (min) and at equilibrium, respectively (mg·g^{-1}); and k_1 is the pseudo-first-order rate constant (min^{-1}).

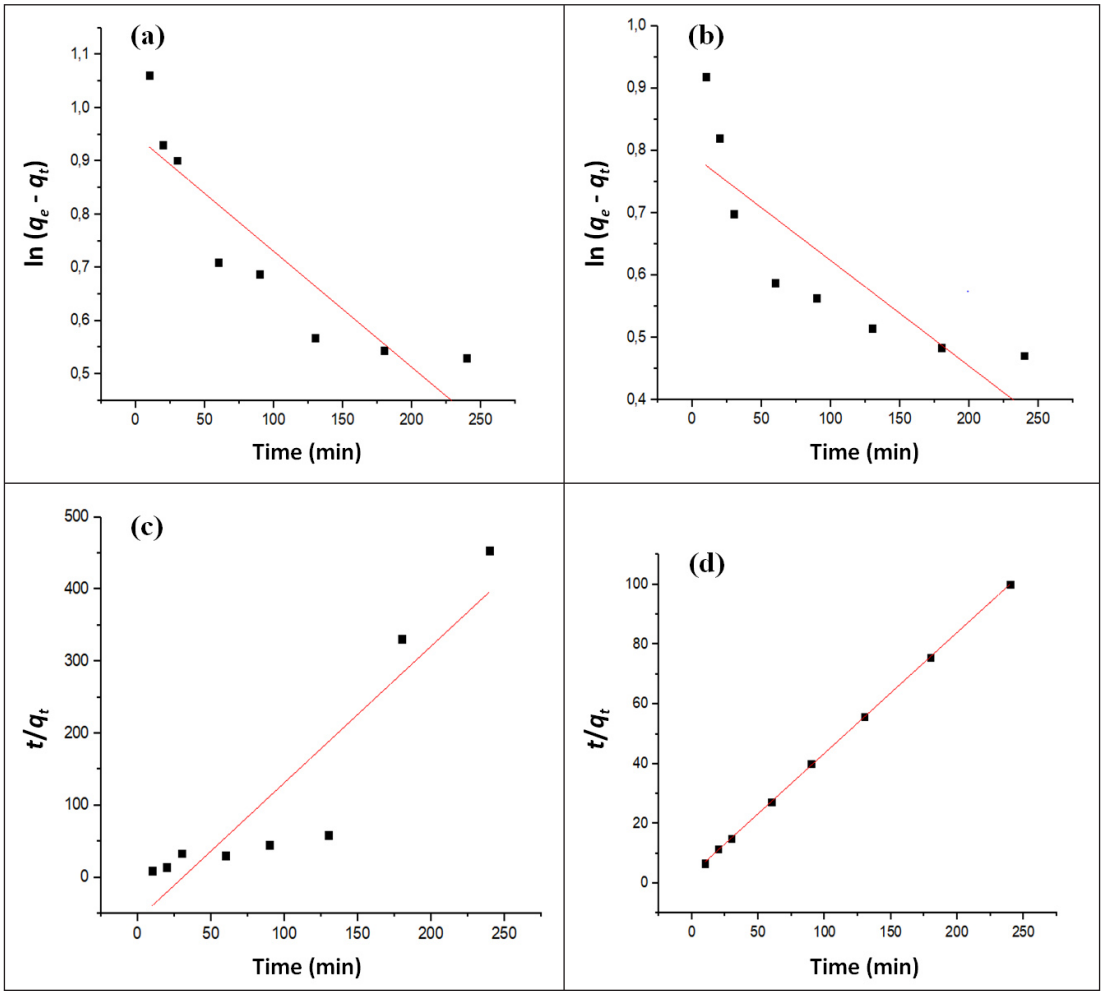

Figure 16. Pseudo-first-order model for (a) MWCNT-COOH, (b) MWCNT-Fe_3O_4 (c) pseudo-second-order model for MWCNT-COOH, and (d) pseudo-second-order model for MWVNT-Fe_3O_4. Experimental conditions: 0.1 g functionalized carbon nanotubes; 60 min reaction time, at temperature 298 K.

Table 4. Pseudo-first-order and pseudo-second-order kinetic parameters for the removal of Pb^{2+}

Adsorbent	Kinetic parameters					
	Pseudo-first-order			Pseudo-second-order		
	k_1 (min^{-1})	q_{e1} ($mg \cdot g^{-1}$)	R^2	k_2 ($g \cdot mg^{-1} \cdot min^{-1}$)	q_e^2 ($mg \cdot g^{-1}$)	R^2
MWCNT-COOH	9.042 x 10^{-6}	2.581	0.771	4.762 x 10^{-3}	0.527	0.816
MWCNT-Au/Fe_3O_4	7.083 x 10^{-6}	2.210	0.674	0.252	0.319	0.999

The pseudo-second-order model is expressed in both linear and non-linear forms:

$$\frac{t}{q_t} = \frac{1}{k_2 q_{e^2}} + \frac{t}{q_e} \quad (9)$$

$$q_t = \frac{k_2 q_{e^2} t}{1 + k_2 q_{e^2} t} \quad (10)$$

where k_2 is the pseudo-second-order rate constant (min^{-1}). A plot of $\frac{t}{q_t}$ vs t should give a straight line whereby q_e and k_2 can be calculated from the slope and intercept, respectively.

In this study, the pseudo-first-order and pseudo-second-order rate models were employed to evaluate the kinetic parameters of lead adsorption on MWCNT-COOH and MWCNT-Fe_3O_4. Figures 16a and 16b represent the pseudo-first-order kinetic models for MWCNT-COOH and MWCNT-Au/Fe_3O_4 nanocomposite adsorbents, respectively. Figures 16c and 16d depict the pseudo-second-order kinetic models for MWCNT-COOH and MWCNT-Au/Fe_3O_4 nanocomposite adsorbents, respectively. The coefficient of determination (R^2) for the pseudo-first-order and pseudo-second-order for MWCNT-Au/Fe3O4 were 0.674 and 0.999, respectively (Table 4). Pseudo-second-order kinetics was observed to be the model with the best fit for explaining the kinetics of Pb (II) adsorption on MWCNT-Au/Fe_3O_4.

Mechanisms of Pb^{2+} ion adsorption by MWCNT-Au/Fe_3O_4

The mechanisms involved when heavy metals are adsorbed onto carbon adsorbents may include electrostatic interaction, ion exchange and surface complexation. These mechanisms play an important role in heavy metal removal because they are closely related to surface functional groups through formation of binding forces, electrostatic forces and covalent bonding (Yang et al., 2019). The Au/Fe_3O_4 that coated MWCNTs has oxygen, gold and iron groups in its unit. Xu et al. (2008) revealed that oxygen-containing groups of carbon nanotubes, especially hydroxyl and carboxyl groups, behave as ion exchange sites whereby a positively charged Pb (II) ion forms a strong bond with these two functional groups through electrostatic interactions and or hydrogen bonding

(Alizadeh et al., 2016). Moreover, the Van der Waals interactions between carbon atoms in graphite sheets of MWCNTs and positively charged lead ions involves interactions between lead cations and gold/iron oxide species which are important for the removal of Pb (II) ions from aqueous solution (Wang et al., 2007).

CONCLUSION

The gold/iron oxide nanoparticles were successfully synthesized from green tea leaves extract. The green tea leaves extract acted as a reducing agent during the synthesis of iron oxide/gold nanoparticles. The successful synthesis of the nanoparticles was confirmed by techniques such as FTIR, TEM, Raman, and XRD. After the functionalization of CNTs, the surface area increased from 96.705 $m^2 \cdot g^{-1}$ for MWCNT-COOH to 105.027 $m^2 \cdot g^{-1}$ for MWCNT-AU/Fe_3O_4. A high sorption capacity was noticed for MWCNT-Au/Fe_3O_4 as compared to the MWCNT-COOH. The optimum pH was 7 with a maximum Pb^{2+} removal percentage of 61.25% and 69.5% for MWCNT-COOH and MWCNT-Au/Fe_3O_4, respectively. The Pb^{2+} removal percentage increased from 50% to 78% with an increase in MWCNT-Au/Fe_3O_4 dosage from 0.02 to 0.1 g. Adsorption isotherm data fitted the Langmuir isotherm and the pseudo-second-order model best described the kinetics of adsorption. The application of MWCNT-Au/Fe_3O_4 showed increased potential for the removal of Pb^{2+} compared to MWCNT-COOH. This indicates that the surface coating of CNTs with the synthesized green nanoparticles enhanced the adsorption capacity of the nanocomposite adsorbent during the removal of Pb (II) ions from wastewater. This study has successfully developed a proof-of-concept to synthesize an eco-friendly nanocomposite for the possible removal of heavy metals from industries. Therefore, MWCNT-Au/Fe_3O_4 can act as a good and efficient adsorbent for the removal of lead (II) ions from wastewater.

AUTHOR CONTRIBUTIONS

Conceptualization by KM and BZ. The original manuscript draft was by BZ, but all authors contributed to its preparation, review and editing. Experiments performed by BZ and data analyses were carried out by BZ in discussion with OS. Supervision by KM and GSS with project administration by KM. All authors have read and agreed to the published version of the manuscript.

CONFLICT OF INTEREST

The authors declare no conflict of interest.

ACKNOWLEDGMENTS

The authors are grateful for the financial support provided by National Research Fund (NRF) and BP Education Foundation SA.

REFERENCES

ABHARI PS, MANTEGHI F and TEHRANI Z (2020) Adsorption of lead ions by green AC/HKUST-1 nanocomposite. *Nanomaterials.* **10** (9) 1674. https://doi.org/10.3390/nano10091647

ADEBWALE K, EGBEDINA A and SHONDE B (2020) Adsorption of lead ions on magnetically separable Fe_3O_4 watermelon composite. *Appl. Water Sci.* **10** (10) 1–8. https://doi.org/10.1007/s13201-020-01307-y

ALGUACIL FJ, ALCARAZ L, GARCÍA-DÍAZ I and LÓPEZ FA (2018) Removal of Pb^{2+} in wastewater via adsorption onto an activated carbon produced from winemaking waste. *Metals.* **8** (9) 697. https://doi.org/10.3390/met8090697

ALKHUDHIRI A, HAKAMI M, ZACHAROF MP, ABU HOMOD H and ALSADUN A (2020) Mercury, arsenic and lead removal by air gap membrane distillation: experimental study. *Water.* **12** (6) 1574. https://doi.org/10.3390/w12061574

ALIZADEH B, GHORBANI M and SALEHI MA (2016) Application of polyrhodanine modified multi-walled carbon nanotubes for high efficiency removal of Pb (II) from aqueous solution. *J. Mol. Liquids.* **220** 142–149. https://doi.org/10.1016/j.molliq.2016.04.065

AKOJI JN (2019) Adsorption performance of packed bed column for the removal of lead (ii) using velvet tamarind (*Dialium indum*) shells. *Asian J. Appl. Chem. Res.* **3** 1–14. https://doi.org/10.9734/ajacr/2019/v3i230089

AKPOR OB and MUCHIE M (2010) Remediation of heavy metals in drinking water and wastewater treatment systems: Processes and applications. *Int. J. Phys. Sci.* **5** (12) 1807–1817.

APPEL C, MA LQ, RHUE RD and KENNELLEY E (2003) Point of zero charge determination in soils and minerals via traditional methods and detection of electroacoustic mobility. *Geoderma.* **113** (1–2) 77–93. https://doi.org/10.1016/S0016-7061(02)00316-6

ARBABI M, HEMATI S and AMIRI M (2015) Removal of lead ions from industrial wastewater: A review of Removal methods. *Int. J. Epidemiol. Res.* **2** (2) 105–109.

ARUNLERTAREE C, KAEWSOMBOON W, KUMSOPA A, POKETHITIYOOK P and PANYAWATHANAKIT P (2007) Removal of lead from battery manufacturing wastewater by egg shell. *Songklanakarin J. Sci. Technol.* **29** (3) 857–868.

ASLAM MMA, KUO HW, DEN W, USMAN M, SULTAN M and ASHRAF H (2021) Functionalized carbon nanotubes (CNTs) for water and wastewater treatment: preparation to application. *Sustainability.* **13** (10) 5717. https://doi.org/10.3390/su13105717

AZIZI S, MAHDAVI SHAHRI M and MOHAMAD R (2017) Green synthesis of zinc oxide nanoparticles for enhanced adsorption of lead ions from aqueous solutions: Equilibrium, kinetic and thermodynamic studies. *Molecules.* **22** (6) 831. https://doi.org/10.3390/molecules22060831

BAO WW, ZOU HF, GAN SC, XU XC, JI GJ and ZHENG KY (2013) Adsorption of heavy metal ions from aqueous solutions by zeolite based on oil shale ash: Kinetic and equilibrium studies. *Chem. Res. Chin. Univ.* **29** (1) 126–131. https://doi.org/10.1007/s40242-013-2139-2

BARAKAT MA (2011) New trends in removing heavy metals from industrial wastewater. *Arab. J. Chem.* **4** (4) 361–377. https://doi.org/10.1016/j.arabjc.2010.07.019

BINDHU MR, REKHA PV, UMAMAHESWARI T and UMADEVI M (2014) Antibacterial activities of Hibiscus cannabinus stem-assisted silver and gold nanoparticles. *Mater. Lett.* **131** 194–197. https://doi.org/10.1016/j.matlet.2014.05.172

BOUDRAHEM F, AISSANI-BENISSAD F and SOUALAH A (2011) Adsorption of lead (II) from aqueous solution by using leaves of date trees as an adsorbent. *J. Chem. Eng. Data.* **56** (5) 1804–1812. https://doi.org/10.1021/je100770j

BURAKOV AE, GALUNIN EV, BURAKOVA IV, KUCHEROVA AE, AGARWAL S, TKACHEV AG and GUPTA VK (2018). Adsorption of heavy metals on conventional and nanostructured materials for wastewater treatment purposes: A review. *Ecotoxicol. Environ. Saf.* **148** 702–712. https://doi.org/10.1016/j.ecoenv.2017.11.034

DAWAGREH AKM, HAILAT M and ALKHASAWNEH H (2017) Evaluation of natural zeolite as sorbent material for the removal of lead from waste water. *Pollut. Res.* **36** (4) 67–74.

DEHAGHI M (2014) Removal of lead ions from aqueous solution using multi-walled carbon nanotubes: The effect of functionalization. *J. Appl. Environ. Biol. Sci.* **4** (2) 316–326.

DE JESÚS RUÍZ-BALTAZAR Á (2021) Sonochemical activation-assisted biosynthesis of Au/Fe_3O_4 nanoparticles and sonocatalytic degradation of methyl orange. *Ultrasonics Sonochem.* **73** 105521. https://doi.org/10.1016/j.ultsonch.2021.105521

ELBOUGHDIRI N (2020) The use of natural zeolite to remove heavy metals Cu (II), Pb (II) and Cd (II), from industrial wastewater. *Cogent Eng.* **7** (1) 1782623. https://doi.org/10.1080/23311916.2020.1782623

ELHAM A, HOSSEIN T and MAHNOOSH H (2010) Removal of Zn (II) and Pb (II) ions using rice husk in food industrial wastewater. *J. Appl. Sci. Environ. Manage.* **14** (4) 159–162. https://doi.org/10.4314/jasem.v14i4.63306

ELMI F, HOSSEINI T, TALESHI MS and TALESHI F (2017) Kinetic and thermodynamic investigation into the lead adsorption process from wastewater through magnetic nanocomposite Fe_3O_4/CNT. *Nanotechnol. Environ. Eng.* **2** (1) 1–13. https://doi.org/10.1007/s41204-017-0023-x

FAYEMI OE, ADEKUNLE AS and EBENSO EE (2015) Metal oxide nanoparticles/multi-walled carbon nanotube nanocomposite modified electrode for the detection of dopamine. Comparative electrochemical study. *J. Biosens. Bioelectrons.* **6** (4) 1–14. https://doi.org/10.4172/2155-6210.1000190

FAYEMIWO OM, DARAMOLA MO and MOOTHI K (2018) Tannin-based adsorbents from green tea for removal of monoaromatic hydrocarbons in water: Preliminary investigations. *Chem. Eng. Commun.* **205** (4) 549–556. https://doi.org/10.1080/00986445.2017.1409738

FODJO EK, GABRIEL KM, SERGE BY, LI D, KONG C and TROKOUREY A (2017) Selective synthesis of Fe_3O_4AuxAgy nanomaterials and their potential applications in catalysis and nanomedicine. *Chem. Centr. J.* **11** (1) 1–9. https://doi.org/10.1186/s13065-017-0288-y

GOTTIMUKKALA KSV, HARIKA RP and ZAMARE D (2017). Green synthesis of iron nanoparticles using green tea leaves extract. *J. Nanomed. Biotherap. Discovery.* **7** 151. https://doi.org/10.4172/2155-983X.1000151

GUSAIN R, KUMAR N, FOSSO-KANKEU E and RAY SS (2019) Efficient removal of Pb (II) and Cd (II) from industrial mine water by a hierarchical MoS2/SH-MWCNT nanocomposite. *ACS Omega.* **4** (9) 13922–13935. https://doi.org/10.1021/acsomega.9b01603

HAIDER AJ, MOHAMMED MR and AHMED DS (2014) Preparation and characterization of multi walled carbon nanotubes/Ag nanoparticles hybrid materials. *Int. J. Sci. Eng. Res.* **5** (3) 255–261.

HAMZA IA, MARTINCIGH BS, NGILA JC and NYAMORI VO (2013) Adsorption studies of aqueous Pb(II) onto a sugarcane bagasse/multi-walled carbon nanotube composite. *Phys. Chem. Earth A/B/C.* **66** 157–166. https://doi.org/10.1016/j.pce.2013.08.006

HASSAN KH and MAHDI ER (2016) Synthesis and characterization of copper, iron oxide nanoparticles used to remove lead from aqueous solution. *Asian J. Appl. Sci.* **4** (3).

HAYATI B, MALEKI A, NAJAFI F, DARAEI H, GHARIBI F and MCKAY G (2016) Synthesis and characterization of PAMAM/CNT nanocomposite as a super-capacity adsorbent for heavy metal (Ni^{2+}, Zn^{2+}, As^{3+}, Co^{2+}) removal from wastewater. *J. Mol. Liq.* **224** 1032–1040. https://doi.org/10.1016/j.molliq.2016.10.053

ISLAM MS, KURAWAKI J, KUSUMOTO Y, ABDULLA-AL-MAMUN M and MUKHLISH MB (2012) Hydrothermal novel synthesis of neck-structured hyperthermia-suitable magnetic (Fe_3O_4, γ-Fe_2O_3 and α-Fe_2O_3) nanoparticles. *J. Sci. Res.* **4** (1) 99–99. https://doi.org/10.3329/jsr.v4i1.8727

KANAMARLAPUDI SLRK, CHINTALPUDI VK and MUDDADA S (2018) Application of biosorption for removal of heavy metals from wastewater. *Biosorption.* **18** 69–116. https://doi.org/10.5772/intechopen.77315

KHARISSOVA OV, DIAS HR, KHARISOV BI, PÉREZ BO and PÉREZ VMJ (2013) The greener synthesis of nanoparticles. *Trends Biotechnol.* **31** (4) 240–248. https://doi.org/10.1016/j.tibtech.2013.01.003

KULKARNI SJ (2016) Wastewater treatment for lead removal: a review. *Int. J. Sci. Res. Sci. Eng. Technol.* **1** (1) 272–275.

LI Y, HE J, ZHANG K, LIU T, HU Y, CHEN X, WANG C, HUANG X, KONG L and LIU J (2019) Super rapid removal of copper, cadmium and lead ions from water by NTA-silica gel. *RSC Adv.* **9** (1)397-407.

LIU Y, YAN J, YUAN D, LI Q and WU X (2013) The study of lead removal from aqueous solution using an electrochemical method with a stainless steel net electrode coated with single wall carbon nanotubes. *Chem. Eng. J.* **218** 81–88. https://doi.org/10.1016/j.cej.2012.12.020

LU C and CHIU H (2008) Chemical modification of multiwalled carbon nanotubes for sorption of Zn2+ from aqueous solution. *Chem. Eng. J.* **139** (3) 462–468. https://doi.org/10.1016/j.cej.2007.08.013

MAHMUD HNME, HOSSEINI S and YAHYA R (2014) Polymer adsorbent for the removal of lead ions from aqueous solution. *Int. J. Technical Res. Appl.* **11** 04–08.

MAHMOUD AED, AL-QAHTANI KM, ALFLAIJ SO, AL-QAHTANI SF and ALSAMHAN FA (2021) Green copper oxide nanoparticles for lead, nickel, and cadmium removal from contaminated water. *Sci. Rep.* **11** (1) 1–13.

MÉNESI J, KÖRÖSI L, BAZSÓ É, ZÖLLMER V, RICHARDT A and DÉKÁNY I (2008) Photocatalytic oxidation of organic pollutants on titania–clay composites. *Chemosphere.* **70** (3) 538–542. https://doi.org/10.1016/j.chemosphere.2007.06.049

NITTI F (2014) Synthesis of gold nanoparticles and their application for detection and removal of water contaminants. *Media Sains.* **13** (2) 221–232.

NOSAKA Y, MATSUSHITA M, NISHINO J and NOSAKA AY (2005) Nitrogen-doped titanium dioxide photocatalysts for visible response prepared by using organic compounds. *Sci. Technol. Adv. Mater.* **6** (2) 143. https://doi.org/10.1016/j.stam.2004.11.006

NWABANNE JTand IGBOKWE PK (2012) Adsorption performance of packed bed column for the removal of lead (II) using oil palm fibre. *Int. J. Appl. Sci. Technol.* **2** (5) 106–115.

OKOLO BI, OKE EO, AGU CM, ADEYI O, NWOSO-OBIEOGU K and AKATOBI KN (2020) Adsorption of lead (II) from aqueous solution using Africa elemi seed, mucuna shell and oyster shell as adsorbents and optimization using Box–Behnken design. *Appl. Water Sci.* **10** (8) 1–23. https://doi.org/10.1007/s13201-020-01242-y

ORLOV A, JEFFERSON DA, TIKHOV M and LAMBERT RM (2007) Enhancement of MTBE photocatalytic degradation by modification of TiO_2 with gold nanoparticles. *Catal. Commun.* **8** (5) 821–824. https://doi.org/10.1016/j.catcom.2006.08.040

OUNI L, RAMAZANI A and FARDOOD ST (2019) An overview of carbon nanotubes role in heavy metals removal from wastewater. *Front. Chem. Sci. Eng.* **13** 274–295. https://doi.org/10.1007/s11705-018-1765-0

OYETADE OA, NYAMORI VO, MARTINCIGH BS and JONNALAGADDA SB (2016) Nitrogen-functionalised carbon nanotubes as a novel adsorbent for the removal of Cu (II) from aqueous solution. *RSC Adv.* **6** (4) 2731–2745. https://doi.org/10.1039/C5RA23900A

PANDEY PK, SHARMA SK and SAMBI SS (2015) Removal of lead (II) from waste water on zeolite-NaX. *J. Environ. Chem. Eng.* **3** (4) 2604–2610. https://doi.org/10.1016/j.jece.2015.09.008

PANDHARE G, TRIVEDI N, PATHRABE R and DAWANDE SD (2013) Adsorption of cadmium (II) and lead (II) from a stock solution using neem leaves powder as a low-cost adsorbent. *Int. J. Innovative Res. Sci. Eng. Technol.* **2** (10) 5752–5761.

POHL A (2020) Removal of heavy metal ions from water and wastewaters by sulphur-containing precipitation agents. *Water Air Soil Pollut.* **231** (10) 1–17. https://doi.org/10.1007/s11270-020-04863-w

PRIYADARSHINI E and PRADHAN N (2017) Gold nanoparticles as efficient sensors in colorimetric detection of toxic metal ions: a review. *Sens. Actuat. B Chem.* **238** 888–902. https://doi.org/10.1016/j.snb.2016.06.081

QIAN H, PRETZER LA, VELAZQUEZ JC, ZHAO Z and WONG MS (2013) Gold nanoparticles for cleaning contaminated water. *J. Chem. Technol. Biotechnol.* **88** (5) 735–741.

RODRÍGUEZ C, BRIANO S and LEIVA E (2020) Increased adsorption of heavy metal ions in multi-walled carbon nanotubes with improved dispersion stability. *Molecules.* **25** (14) 3106. https://doi.org/10.3390/molecules25143106

SADARE OO and DARAMOLA MO (2019) Adsorptive removal of dibenzothiophene from petroleum distillates using pomegranate leaf (*Punica granatum*) powder as a greener adsorbent. *Chem. Eng. Commun.* **206** (3) 333–345. https://doi.org/10.1080/00986445.2018.1488691

SADARE OO, AYENI AO and DARAMOLA MO (2020) Performance evaluation of green adsorbent (neem leaf powder) for desulfurization of petroleum distillate. *Chem. Eng. Trans.* **80** 361–366. https://doi.org/10.3303/CET2080061

SARMA GK, GUPTA SS and BHATTACHARYYA KG (2019) Nanomaterials as versatile adsorbents for heavy metal ions in water: a review. *Environ. Sci. Pollut. Res.* **26** (7) 6245–6278. https://doi.org/10.1007/s11356-018-04093-y

SHARMA RK, GULATI S and MEHTA S (2012) Preparation of gold nanoparticles using tea: a green chemistry experiment. *J. Chem. Educ.* **89** (10) 1316–1318. https://doi.org/10.1021/ed2002175

SHARMA S and BHATTACHARYA A (2017) Drinking water contamination and treatment techniques. *Appl. Water Sci.* **7** (3) 1043–1067. https://doi.org/10.1007/s13201-016-0455-7

SKWAREK E, BOLBUKH Y, TERTYKH V and JANUSZ W (2016) Electrokinetic properties of the pristine and oxidized MWCNT depending on the electrolyte type and concentration. *Nanoscale Res. Lett.* **11** (1) 1–17. https://doi.org/10.1186%2Fs11671-016-1367-z

SONI R, PAL AK, TRIPATHI P, LAL JA, KESARI K and TRIPATHI V (2020) An overview of nanoscale materials on the removal of wastewater contaminants. *Appl. Water Sci.* **10** (8) 1–9. https://doi.org/10.1007/s13201-020-01275-3

TAO Y, ZHANG C, LÜ T and ZHAO H (2020) Removal of Pb (II) ions from wastewater by using polyethyleneimine-functionalized Fe_3O_4 magnetic nanoparticles. *Appl. Sci.* **10** (3) 948. https://doi.org/10.3390/app10030948

TEHRANI MS, AZAR PA, EHSANI NAMIN P and DEHAGHI SM (2014) Removal of lead ions from aqueous solution using multi-walled carbon nanotubes: The effect of functionalization. *J. Appl. Environ. Biol. Sci.* **4** 316–326.

THAÇI BS and GASHI ST (2019) Reverse osmosis removal of heavy metals from wastewater effluents using biowaste materials pretreatment. *Pol. J. Environ. Stud.* **28** (1) 337–341. https://doi.org/10.15244/pjoes/81268

TCHOUNWOU PB, YEDJOU CG, PATLOLLA AK and SUTTON DJ (2012) Heavy metal toxicity and the environment. *Mol. Clin. Environ. Toxicol.* **101** 133–164. https://doi.org/10.1007/978-3-7643-8340-4_6

WANG SG, GONG WX, LIU XW, YAO YW, GAO BY and YUE QY (2007) Removal of lead (II) from aqueous solution by adsorption onto manganese oxide-coated carbon nanotubes. *Sep. Purif. Technol.* **58** (1) 17–23. https://doi.org/10.1016/j.seppur.2007.07.006

XU D, TAN X, CHEN C and WANG X (2008) Removal of Pb (II) from aqueous solution by oxidized multiwalled carbon nanotubes. *J. Hazardous Mater.* **154** (1–3) 407–416. https://doi.org/10.1016/j.jhazmat.2007.10.059

YARKANDI NH (2014) Removal of lead (II) from waste water by adsorption. *International J. Curr. Microbiol. Appl. Sci.* **3** (4) 207–228. http://www.ijcmas.com/vol-3-4/Naeema% (Accessed 9 July 2021).

YANG X, WAN Y, ZHENG Y, HE F, YU Z, HUANG J, WANG H, OK YS, JIANG Y and GAO B (2019) Surface functional groups of carbon-based adsorbents and their roles in the removal of heavy metals from aqueous solutions: a critical review. *Chem. Eng. J.* **366** 608–621. https://doi.org/10.1016/j.cej.2019.02.119

ZAFARZADEH A, SADEGHI M, GOLBINI MOFRAD A and BEIRAMI S (2018) Removal of lead by activated carbon and citrus coal from drinking water. *Desalin. Water Treat.* **105** 282–86. https://doi.org/10.5004/dwt.2018.22024

ZEWAIL TM and YOUSEF NS (2015) Kinetic study of heavy metal ions removal by ion exchange in batch conical air spouted bed. *Alexandria Eng. J.* **54** (1) 83–90. https://doi.org/10.1016/j.aej.2014.11.008